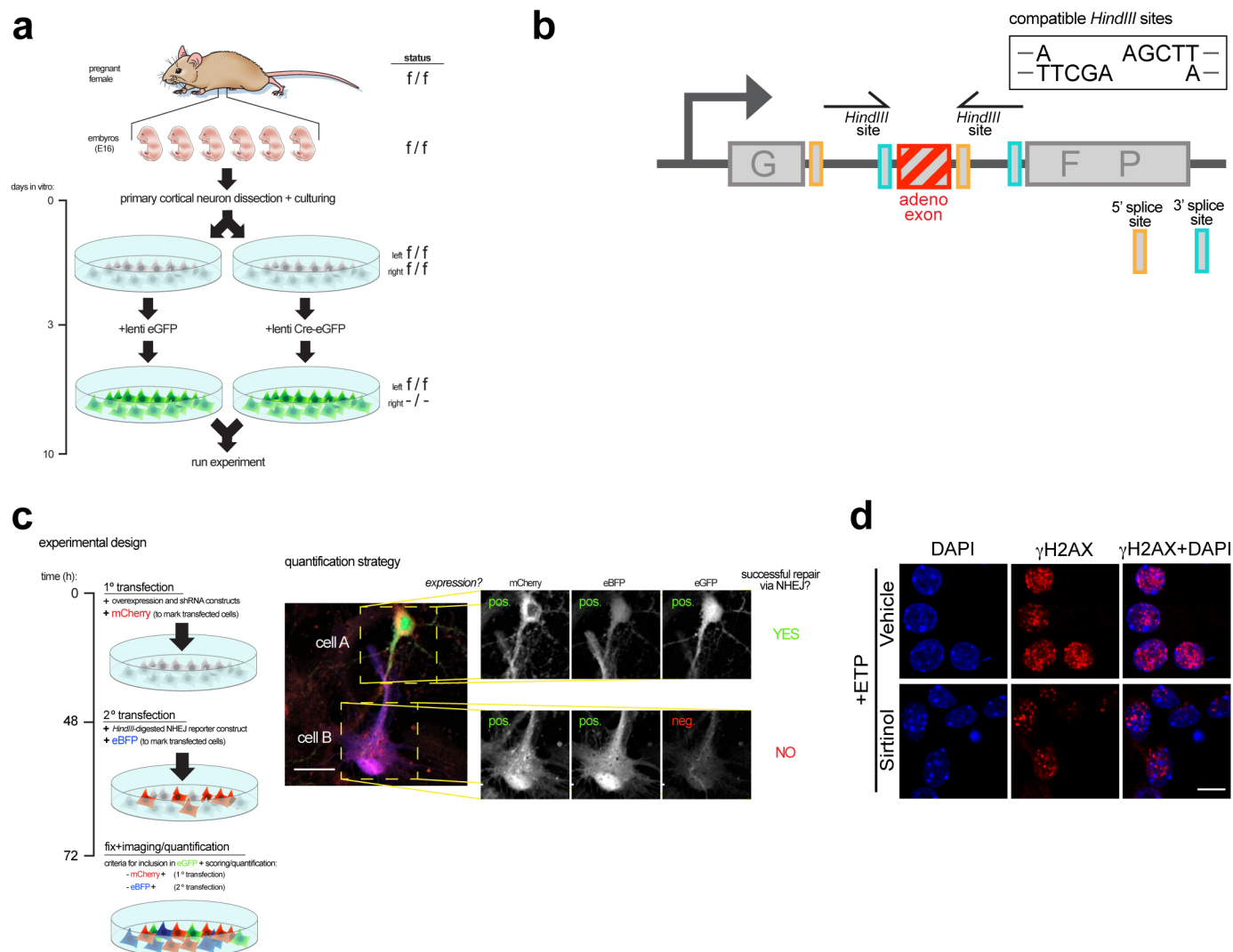
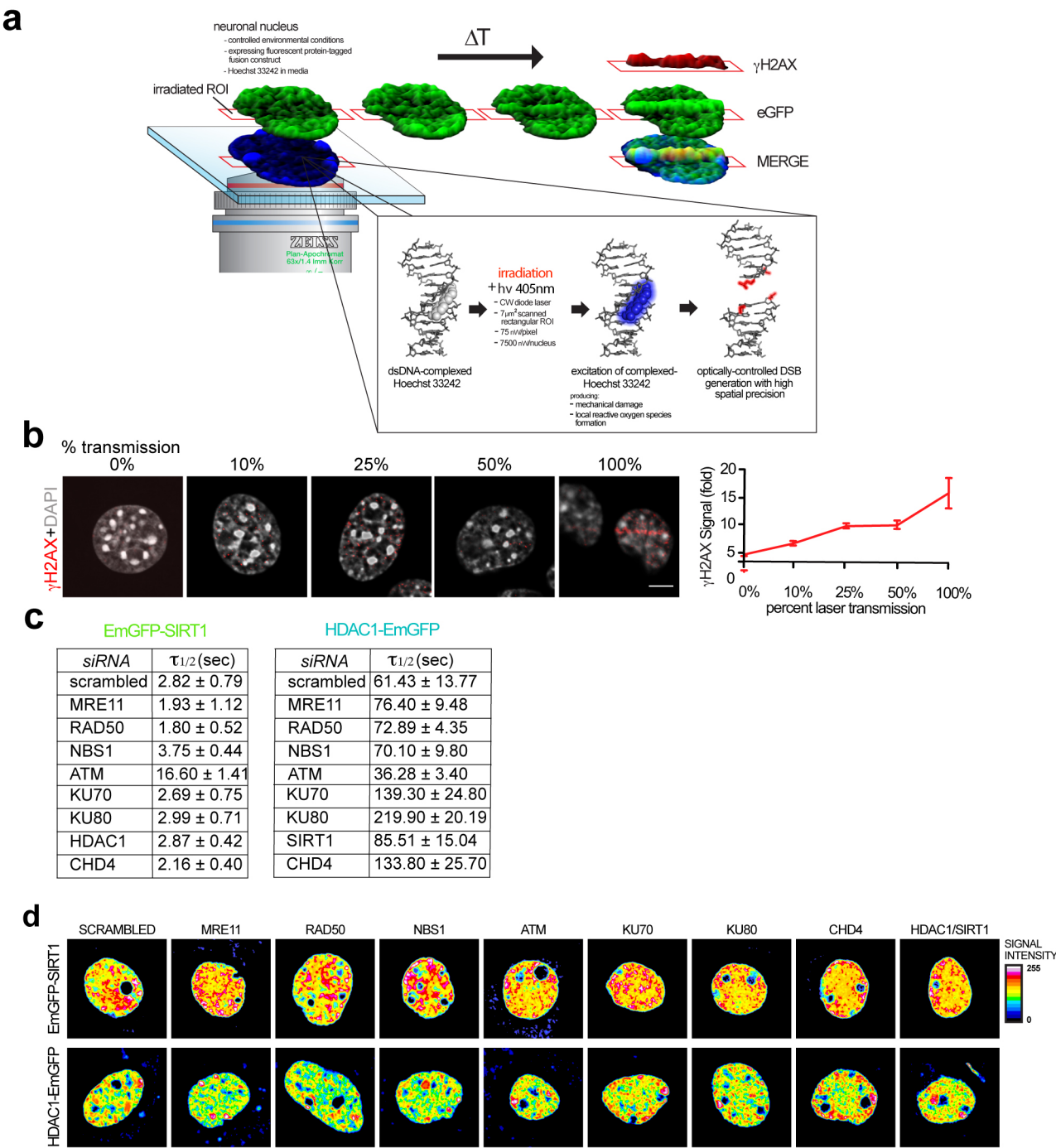


## Supplementary Figure 1



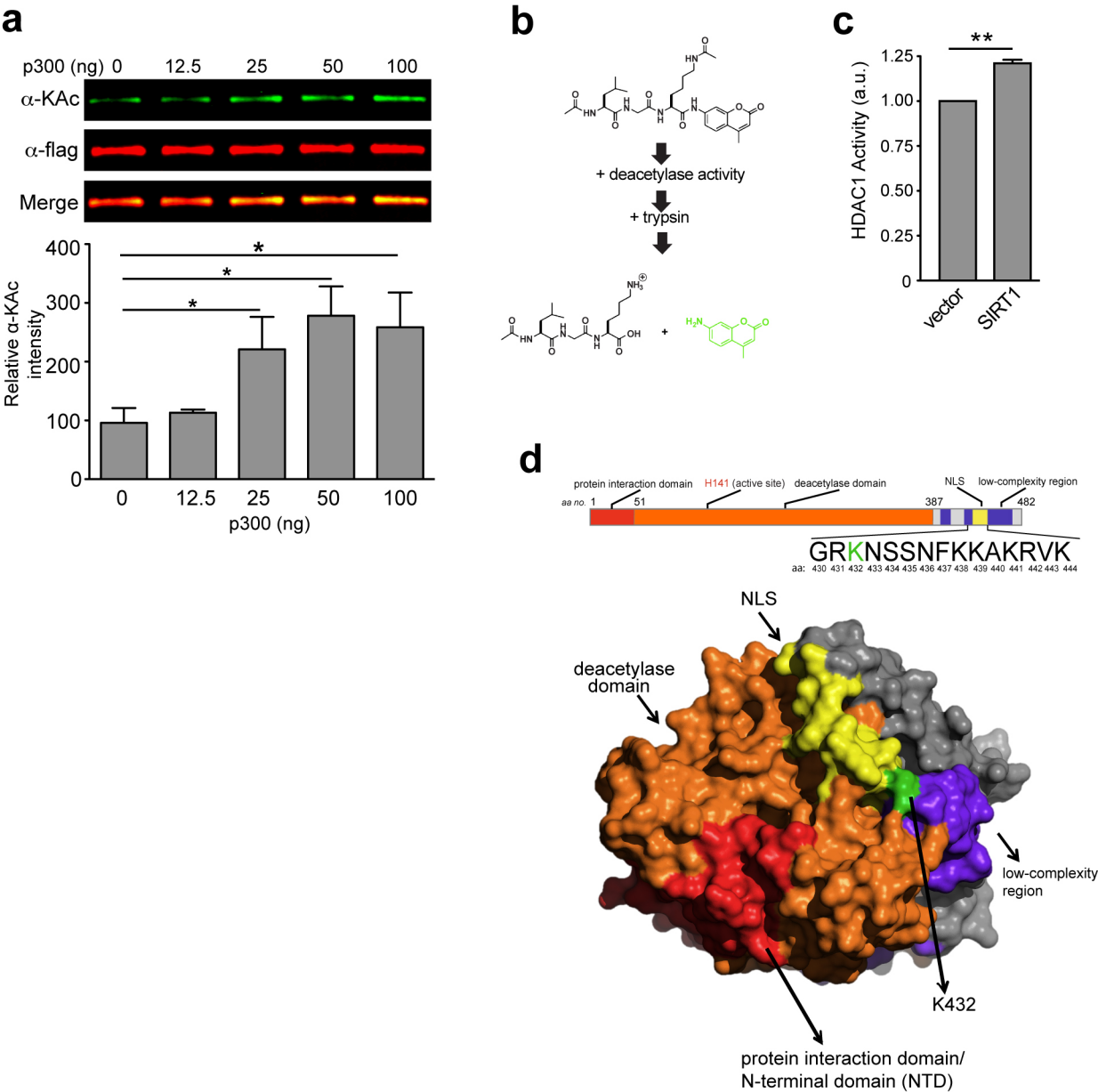
**Supplementary Figure 1. a**, Schematic for generating *Sirt1* KO neurons. Dissociated primary cortical neurons were cultured from E16 *Sirt1* F/F embryos. DIV3 cultures were infected with a lentiviral vector carrying either a functional Cre recombinase (Cre-eGFP) or a non-functional Cre (eGFP). Neurons were usually used 7 days after infection with Cre-eGFP. A similar strategy was used to generate *Hdac1* KO neurons. **b**, Construct used to measure efficiency of DNA repair using NHEJ. In this construct, a functional *eGFP* gene is interrupted by an intron. The presence of an adenoviral exon sequence within the intron prevents it from normally being spliced out. Generation of a DSB using HindIII and its subsequent repair using NHEJ disrupts the adenoviral exon sequence. Consequently, the intron is spliced out, allowing for expression of GFP. In this way, GFP+ cells can be used to score the efficiency of NHEJ. **c**, Outline of the experimental scheme used to adapt the NHEJ reporter assay to cultured primary neurons in our study. **d**, Primary cortical neurons (DIV14) were incubated overnight with the SIRT1 inhibitor, sirtinol (20μM final), then treated with 2μM etoposide for 1 h and analyzed as in Fig. 1c. Scale bar = 10μm.

Supplementary Figure 2



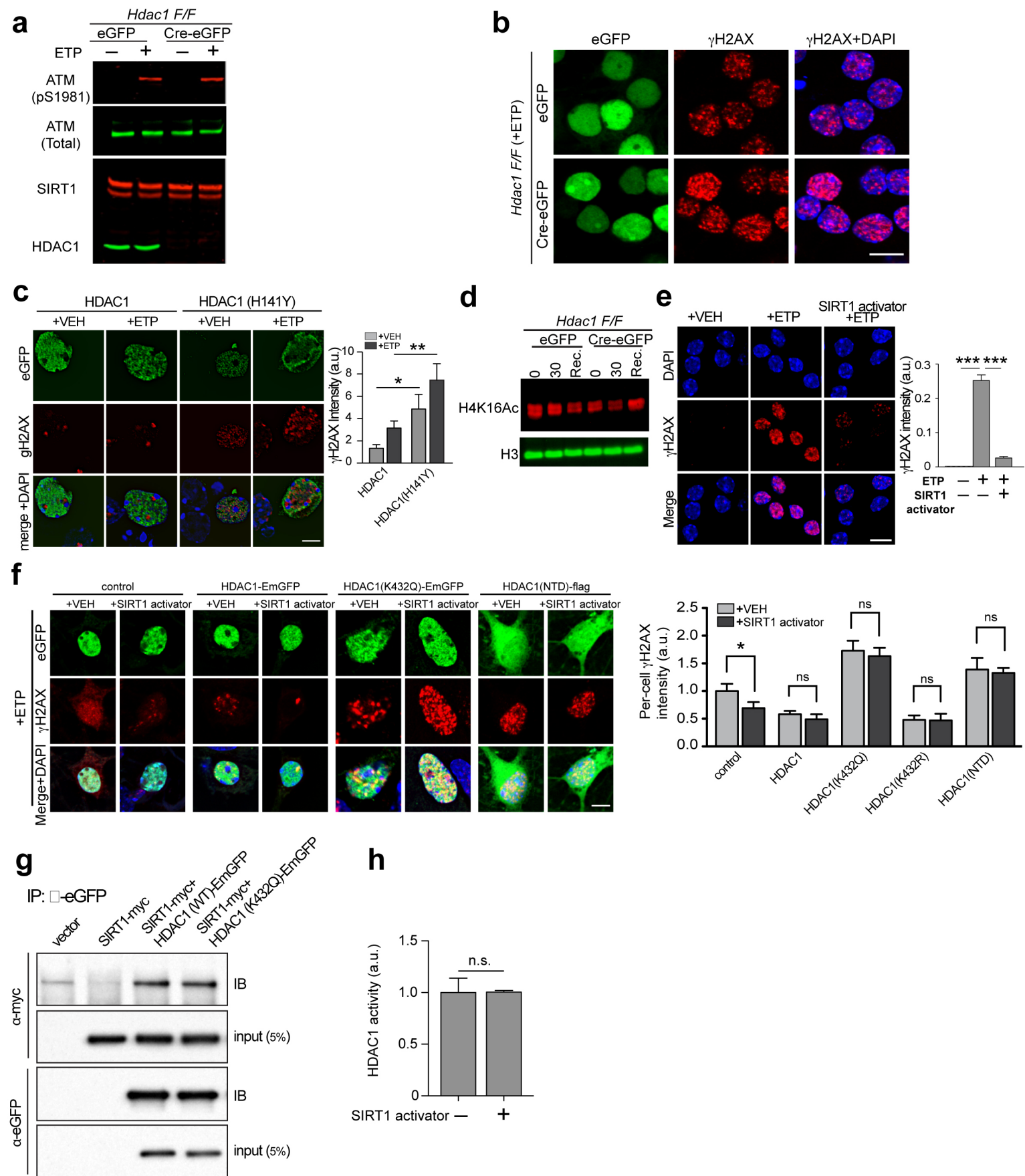
**Supplementary Figure 2. a**, Schematic of laser microirradiation. A Zeiss LSM710 inverted laser scanning confocal microscope equipped with a 405nm diode laser was used to irradiate a thin sub-nuclear strip of Hoechst-stained primary neurons. Localization of proteins to sites of laser-induced DNA DSBs can be monitored as increased fluorescence intensity within lesioned regions as visualized either by immunocytochemistry of fixed cells (for instance,  $\gamma$ H2AX) or through live imaging of cells carrying fluorescently tagged repair proteins. **b**, Serial attenuation of transmitted 405 nm wavelength light emitted from a continuous-wave diode laser yields a dose-dependency in  $\gamma$ H2AX signal intensity within lesion ROIs. ROI area (2μm<sup>2</sup>), laser power (100%), and scan iterations were held constant for Hoechst33242 pre-sensitized neuronal nuclei, while percent transmission was varied as indicated. Neurons were then fixed and stained with  $\gamma$ H2AX. Scale bar = 7μM. **c**, Table indicating the time taken by EmGFP-SIRT1 (left) and HDAC1-EmGFP (right) to attain half-maximal fluorescence intensity in the lesioned region following the knockdown of the DSB components in Fig. 3d. **d**, Representative images of EmGFP-SIRT1 (top) and HDAC1-EmGFP (bottom) expressing neurons that were transfected with the indicated siRNAs to show that the various siRNAs did not affect expression of the two proteins.

**Supplementary Figure 3**



**Supplementary Figure 3. a**, Increasing amounts of p300 were incubated with a fixed amount of HDAC1 and the effect of p300 on the acetylation of HDAC1 was assessed using quantitative western blotting (\*  $p < 0.05$ , one-way ANOVA). **b**, Schematic of a fluorescence-based reporter assay used to measure HDAC1 enzymatic activity. Deacetylation of the substrate sensitizes it to cleavage by trypsin, which results in the release of a fluorescent moiety (green). Fluorescence intensity is thus used as an indicator of deacetylase activity. **c**, HEK293T cells were transfected with either an empty vector or a vector carrying SIRT1. HDAC1 was then immunoprecipitated, and its activity was measured as described in b (\* $p < 0.01$ , unpaired t-test). **d**, Sequence and structural information from an already crystallized HDAC1 ancestor from the hyperthermophilic bacterium *Aquifex aeolicus* (PMID: 10490031) was used to generate a computational model predicting the tertiary structure of HDAC1. Identical domain color scheme was utilized in domain illustration and predicted structure rendering. Green indicates the position of the lysine residue, K432.

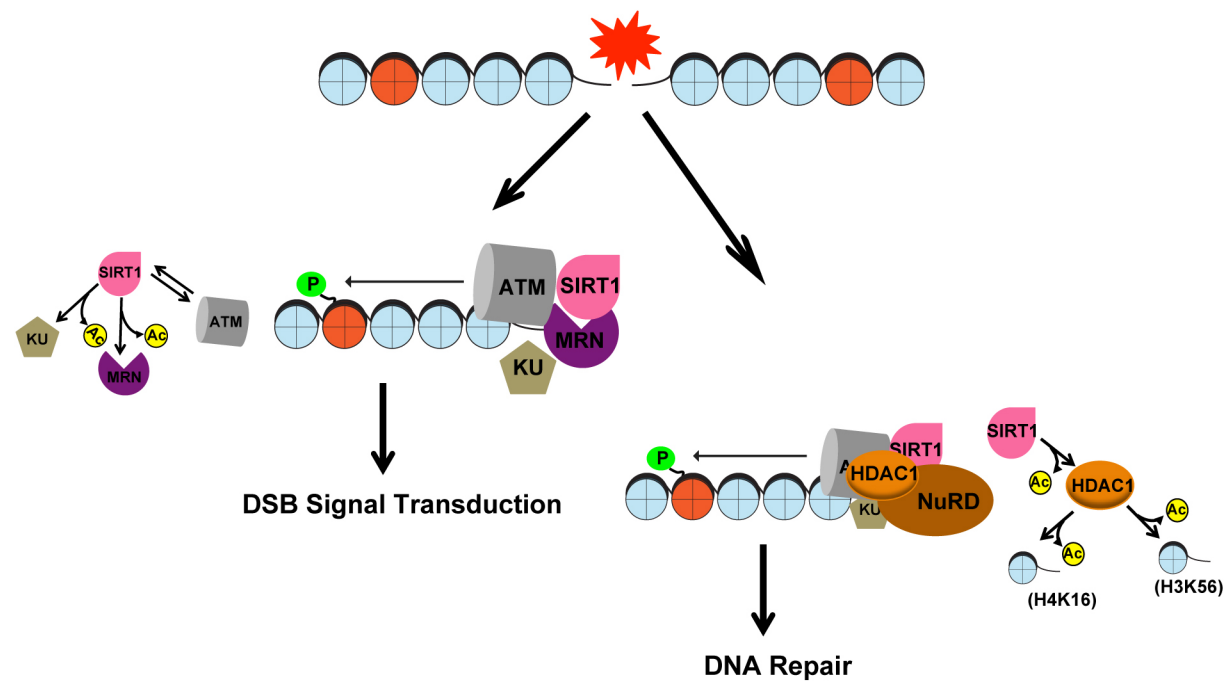
Supplementary Figure 4





**Supplementary Figure 4.** **a**, *Hdac1* *F/F* neurons infected with either eGFP or Cre-eGFP were treated with either vehicle or 5μM etoposide for 1h, following which the cells were lysed and levels of phosphorylated ATM were compared by western blotting. **b**, *Hdac1* *F/F* neurons infected as in **a** were treated with either vehicle or 2μM etoposide for 1h, following which the cells were fixed and stained with antibodies to γH2AX. Per-Cell γH2AX intensity was then quantified. **c**, Mouse primary neurons transfected with the indicated HDAC1 constructs were treated with 2μM etoposide for 1 h, and γH2AX intensity was quantified using per-cell image analysis. Analysis was limited to transfected cells exclusively. Scale bar = 5μm. **d**, *Hdac1* *F/F* neurons were infected as in **a** and treated with 5μM etoposide for 30 min. Cells were then lysed either immediately or following recovery after etoposide washout for an additional 30 min. The lysates were then electrophoresed and processed as in Figure 4c. **e**, Neurons incubated with 10μM compound#10 for 12 h were treated with 5μM etoposide for 1 h, and fixed and stained with antibodies against γH2AX. Graph indicates quantification of γH2AX intensity. Scale bar = 10μm. Quantification shown below (\*\*\*)  $p < 0.001$ , one-way ANOVA). **f**, Cultured primary neurons expressing the indicated proteins were incubated with either vehicle or compound#10. The neurons were then treated with etoposide (2μM) for 1 h, following which the cells were fixed and stained as in Fig. 5d (\*  $p < 0.05$ , one-way ANOVA). **g**, HT22 cells were transfected with the indicated constructs. Cells were then lysed and eGFP-tagged proteins were immunoprecipitated and blotted with antibodies against myc. **h**, The activity of recombinant HDAC1-flag (100ng) incubated either in the presence or absence of the SIRT1 activator, compound#10 (1.1μM final), was measured using a fluorescence-based HDAC enzymatic activity assay as described in Supplementary Fig. 3b.

**Supplementary Figure 5**



**Supplementary Figure 5, Model.** Following DSB formation, DNA ends are recognized by the MRE11 complex and ATM, and DNA end binding by KU70/80 culminates in DSB repair through NHEJ. SIRT1 function is crucial in a number of these early events. SIRT1 is rapidly recruited to DSBs in an ATM-dependent manner and in turn, stabilizes ATM at DSB sites, and stimulates ATM autophosphorylation and the phosphorylation of ATM targets, including H2AX. In addition, SIRT1 also stabilizes NBS1. In this manner, SIRT1 facilitates in transduction of the DSB signal (left arrow). SIRT1 also facilitates DSB repair through its actions on HDAC1, which is recruited to DSBs in a SIRT1-dependent manner. SIRT1-mediated HDAC1 deacetylation allows HDAC1 to target residues such as H4K16Ac and H3K56Ac, whose deacetylation is essential for DNA repair through NHEJ (right arrow).